Supporting Information

Label-free monitoring of drug-induced cytotoxicity and its molecular fingerprint by live-cell Raman and autofluorescence imaging.

Menglu Li[1,2]*, Hao-Xiang Liao[1], Kazuki Bando[1], Yasunori Nawa[1,2], Satoshi Fujita[1,2], Katsumasa Fujita[1,2,3]*

AFFILIATIONS:

[1]Department of Applied Physics, Osaka University, 2-1 Yamadaoka, Suita, Osaka 565-0871, Japan.

[2]AIST-Osaka University Advanced Photonics and Biosensing Open Innovation Laboratory, National Institute of Advanced Industrial Science and Technology (AIST), 2-1 Yamadaoka, Suita, Osaka 565-0871, Japan.

[3]Institute for Open and Transdisciplinary Research Initiatives, Osaka University, 2-1 Yamadaoka, Suita, Osaka 565-0871, Japan.

*Correspondence to: Menglu Li, Katsumasa Fujita

EMAIL: menglu.li@ap.eng.osaka-u.ac.jp, fujita@ap.eng.osaka-u.ac.jp

Table of Contents

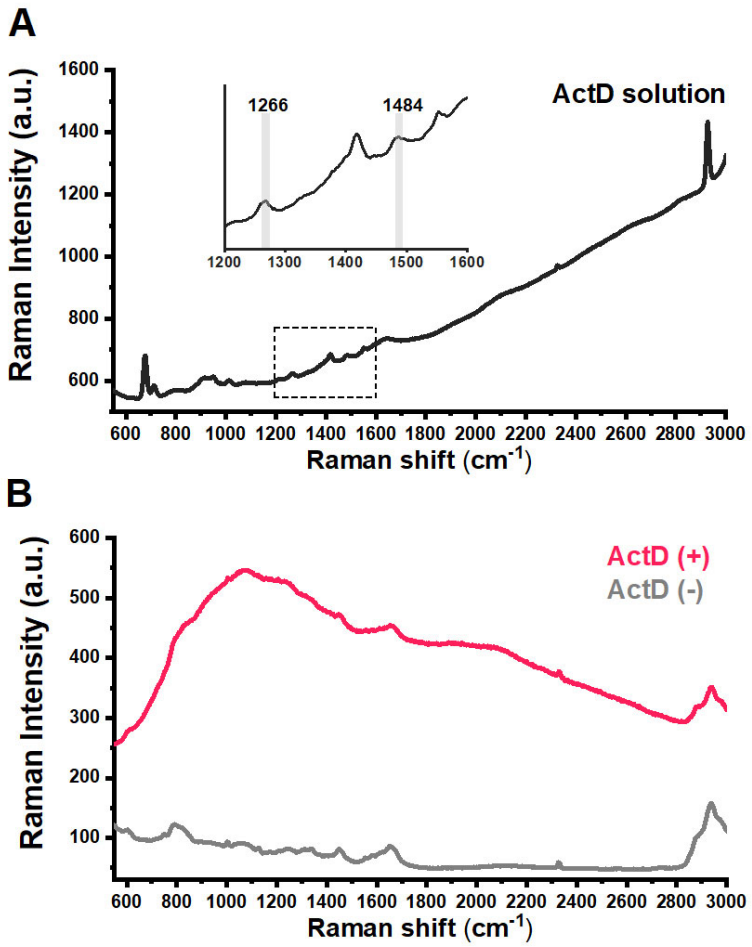

Figure S1. Comparison of the spectrum of ActD in aqueous solution and in cell nuclei. (A) The Raman spectrum of 100 μM ActD in aqueous solution (1% DMSO in PBS). The wavenumber range from 1200-1600 cm^{-1} was enlarged as an insert to show characteristic peaks of ActD in aqueous solution. (B) The spectrum of cell nuclei in the cells treated with 1 μM ActD for 4 h. The peak of this weak fluorescence is at 1149 cm^{-1}, which converted to wavelength is 567 nm. By comparing the spectra of ActD in aqueous solution and in cell nuclei, a blue shift of fluorescence was detected.

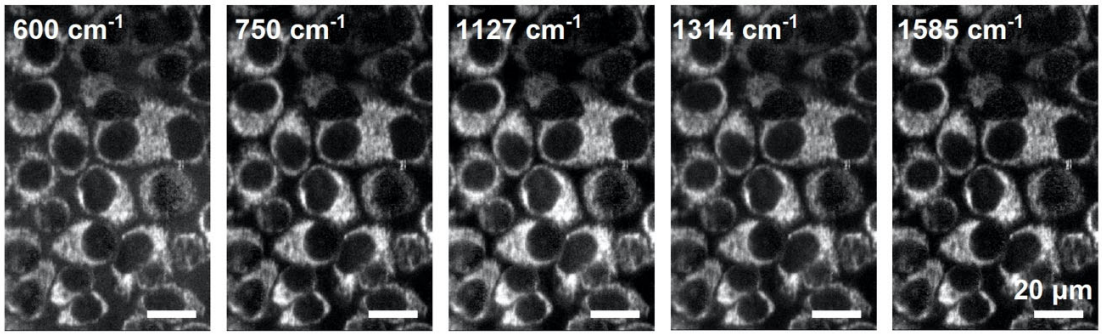

Figure S2. Raman images reconstructed at 600, 750, 1127, 1314, and 1585 cm^{-1}. These Raman shifts can be assigned to the reduced cytochromes. Both reduced cyt *b* and cyt *c* show resonance Raman scattering under 532 nm excitation due to the backbone stretching of porphyrin. This resonant effect enhances the Raman signals of cytochromes compared with other proteins. cyt *b* and cyt *c* shared the same characteristic peaks at 750, 1127, 1314, and 1585 cm^{-1}, but do not share the peak at 600 cm^{-1} (found only from cyt c), which can be used to distinguish cyt *c* from cyt *b*. Since 600 cm^{-1} showed a same tendency compared to 750, 1127, 1314, and 1585 cm^{-1}, the contrast of those images in this measurement considered to be mainly associated with cyt *c*. Scale bars, 50 μm.

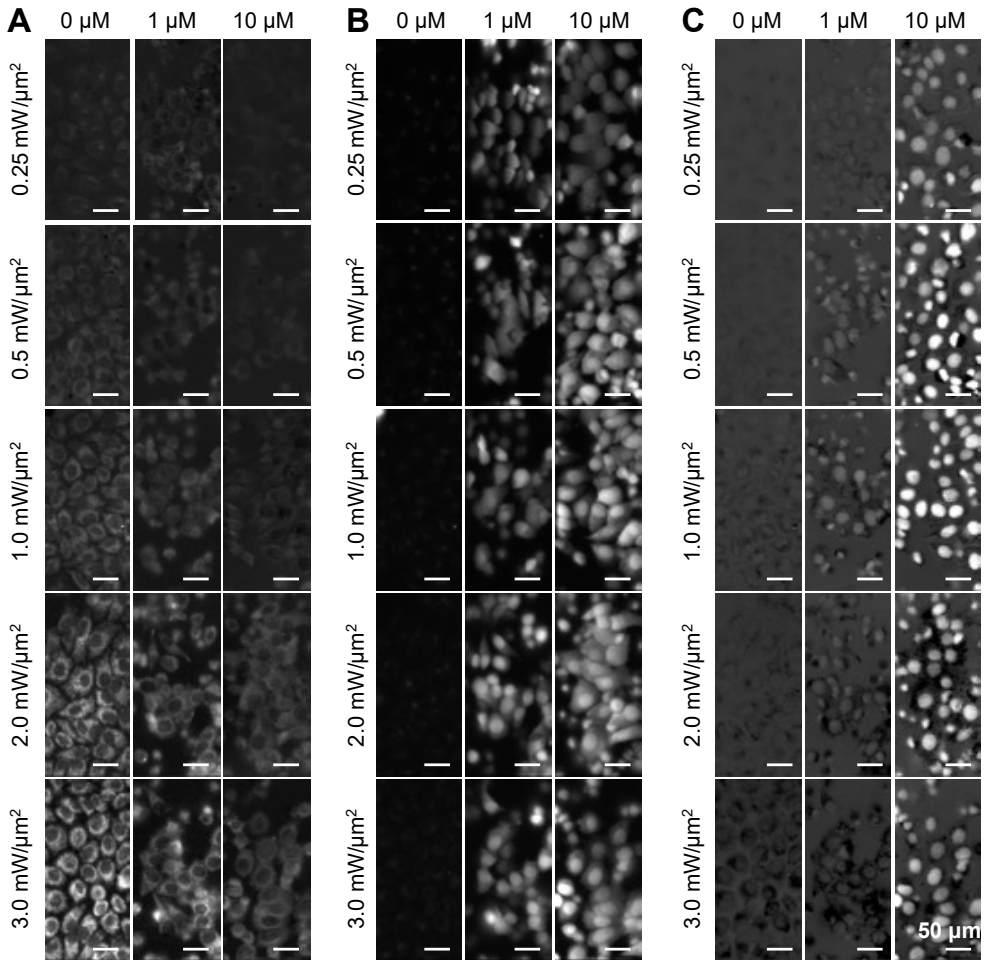

Figure S3. Raman images of cells treated with 0, 1, 10 μM ActD at different power density. (A) Images constructed at 1585 cm^{-1}, which can be assigned to reduced cyt *c*. The dose-dependent decrease in cyt *c* was observed at all power densities, which means the decrease of cyt *c* signal is independent from power density. However, for the signals of ActD, the autofluorescence from 1950-2250 cm^{-1} (B) and the Raman shift at 1484 cm^{-1} (C) showed a similar tendency compared with cyt *c* until 1 mW/um^2. High laser power leads to the decrease of fluorescence and Raman intensity at higher dose of 1 μM and 10 μM. Therefore, 1 $mW/\mu m^2$ was used to observe the conditions of 1 μM and 10 μM ActD. Scale bars, 50 μm.

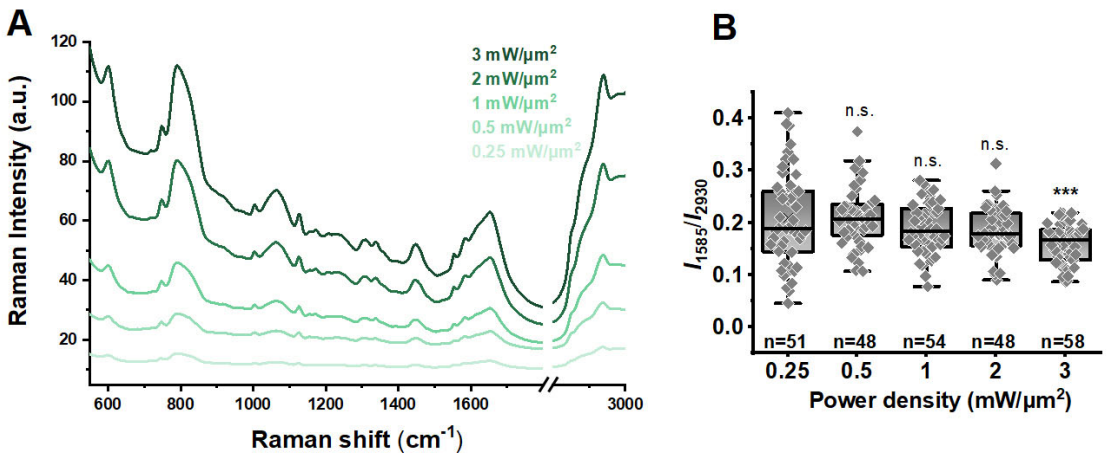

Figure S4. Power density dependency of HeLa cell spectra. (A) Raw spectra of HeLa cells measured at power densities of 0.25, 0.5, 1, 2, 3 mW/μm^2. (B) The normalized Raman intensity of 1585 cm^{-1} to 2930 cm^{-1}. To compare the laser effect on cyt *c* quantitatively, we calculated I_{1585} and I_{2930}, which are the area of Raman peak at 1585 cm^{-1} and 2930 cm^{-1}, respectively, and the ratio of I_{1585} to I_{2930} was used to estimate the effect of laser power on reduced cyt *c* amount. No significant decrease was found until 2 mW/μm^2, and a slight decrease at 3 mW/μm^2 was detected. Therefore, we selected 1 mW/μm^2 for the quantitative analysis. Exposure time of one illumination line was 5s. The box plots illustrate the spread within cell populations (center line, median; box, quartiles; whiskers, 1.5× interquartile range). The significant difference was compared with the most left box. ***: $P < 0.001$; n.s.: $P \geq 0.05$

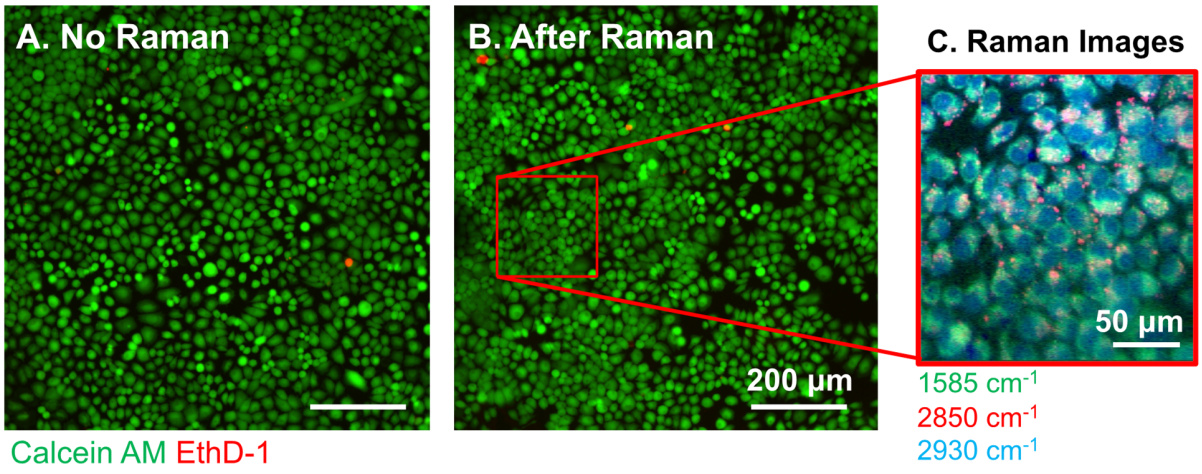

Figure S5. Cell conditions after Raman imaging is evaluated by live/dead assay. (A) Control, cell samples were not observed by Raman microscope. (B) Live/dead assay was performed immediately after the Raman imaging. The Raman imaging area is marked by a red rectangle, and on the right is the color-merged Raman image corresponding to the area indicated by the red rectangle. (C) The Raman images were reconstructed by plotting the peak intensities at 1585 cm^{-1} (green), 2850 cm^{-1} (red), and 2930 cm^{-1} (blue), which can be assigned to cyt *c*, CH_2 symmetric stretching mode, and CH_3 symmetric stretching mode, respectively. The power density is 1 $mW/\mu m^2$ and the exposure time is 5s. To obtain this image, 126 lines were scanned at a pitch size of 1.6 μm. These conditions are the same as those used in the quantitative analysis of this manuscript.

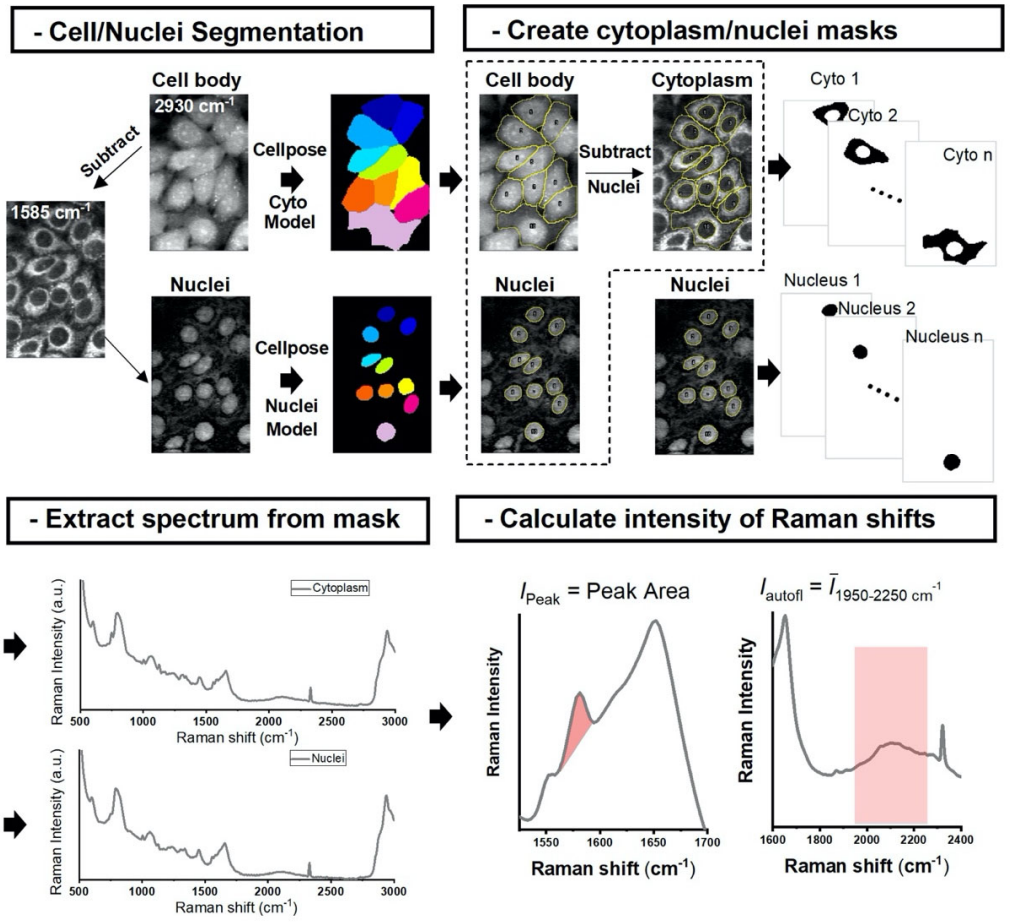

Figure S6. Single cell-based quantification of Raman intensity. Hyperspectral Raman images after SVD were reconstructed, and the Raman shift at 2930 cm^{-1} was utilized for the segmentation of the whole cell body. After subtracting by the contrast at 1585 cm^{-1}, the nuclei image was acquired and used for the segmentation of cell nuclei. Segmentation was automatically performed by Cellpose with manual modifications. The outlines of segmentation were exported to ImageJ, and masks of each segmentation were created. Then, the masks were applied to extract the average spectra in the mask region. The average spectra of the cytoplasm and nucleus in the same cell were obtained. The intensity of the Raman shift was calculated as the area of the peak. The intensity of autofluorescence was measured as the average value from 1950 cm^{-1} to 2250 cm^{-1}.

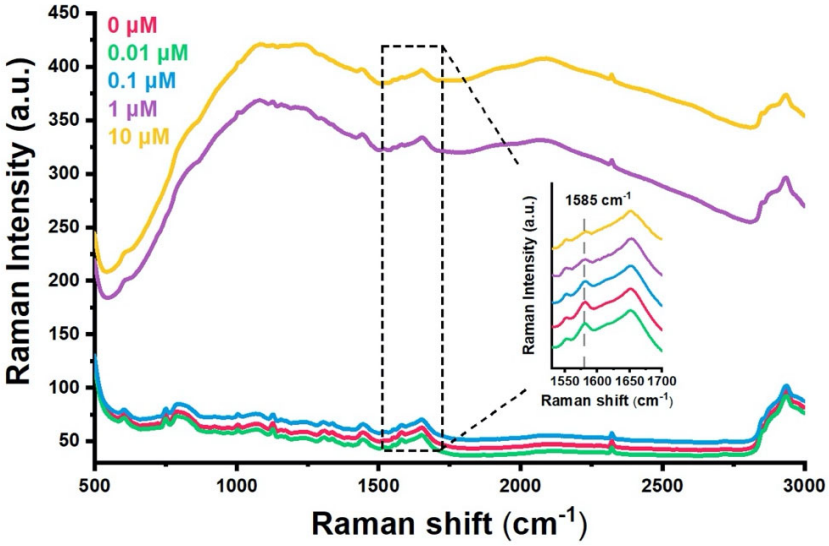

Figure S7. The complete spectra of HeLa cells treated with different concentration of ActD. At 1 μM and 10 μM ActD, a broad fluorescence background was elevated due to ActD treatment. The enlarged Raman spectra from 1530 cm^{-1} to 1700 cm^{-1} with the same vertical scale were shown as an insert.

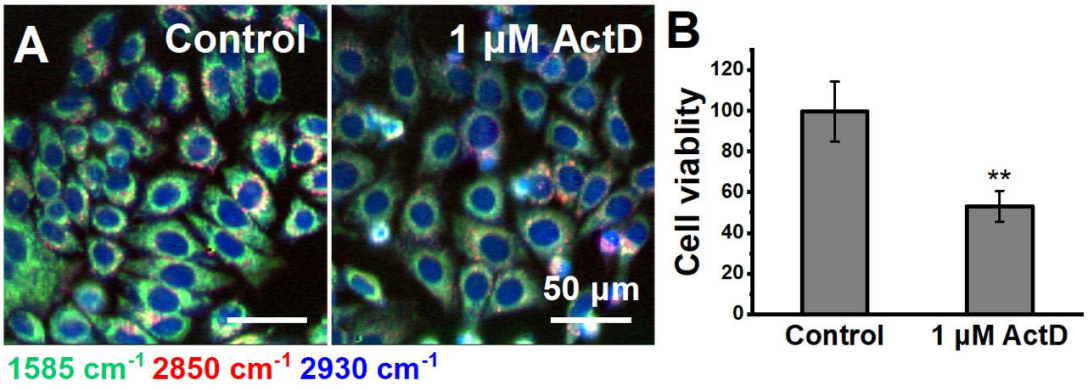

Figure S8. Raman hyperspectral images of HeLa cells treated with 1 μM ActD for 1 h and 6 h post-incubation with fresh medium. The HeLa cells without treatment with ActD were taken as controls. (A) Raman images reconstructed at 1585 cm^{-1}, 2850 cm^{-1}, and 2930 cm^{-1}, which can be assigned to cyt *c*, lipids, and CH_3 symmetric stretching mode. The power density is 1 $mW/\mu m^2$. Scale bars, 50 μm. (B) Cell viability measured by the MTT assay. **: $P < 0.01$.

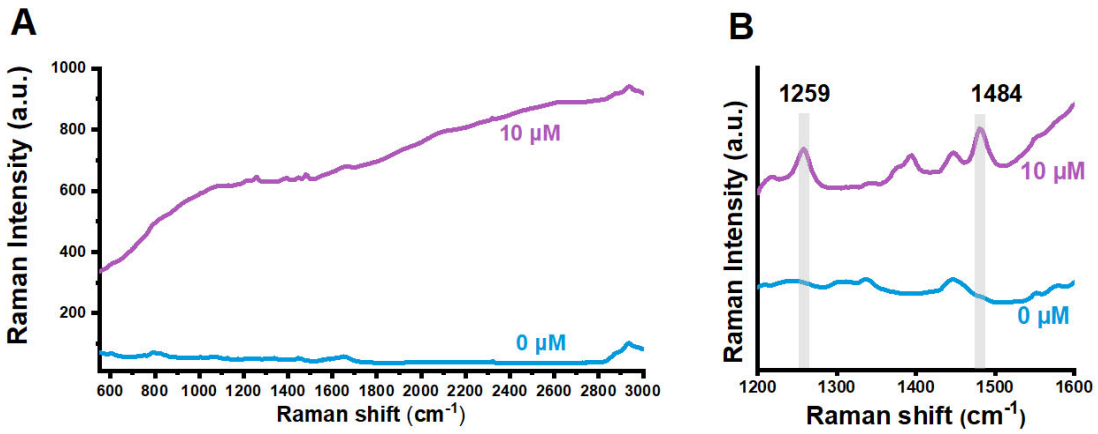

Figure S9. Comparison of the average spectra of nuclei in cells treated with 0 μM and 10 μM ActD. (A) Raw spectra with residual background caused by autofluorescence of ActD. (B) A narrow optical window with the same vertical scale to compare changes in the characteristic peaks of ActD.

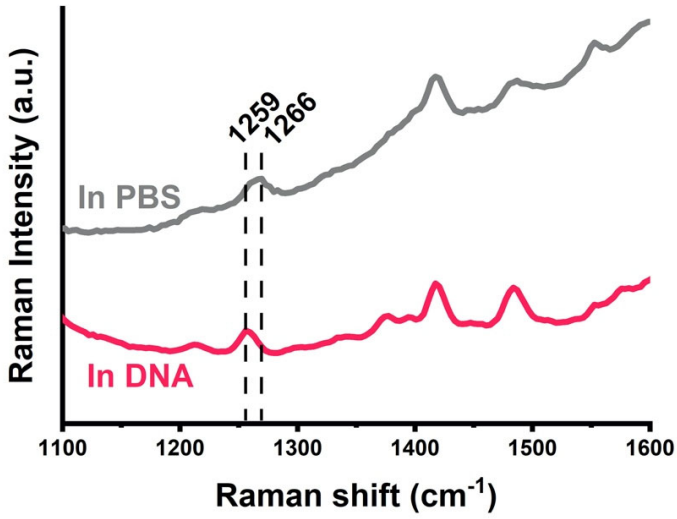

Figure S10. The Raman shifts after ActD binds to DNA. Raman spectrum of 100 μM ActD in PBS (black trace) and in 10 mg/ml DNA solution (red trace). A shift of 1266 cm^{-1} to 1259 cm^{-1} was identified which supports that the same shift observed in cell nuclei is due to ActD binding to DNA.

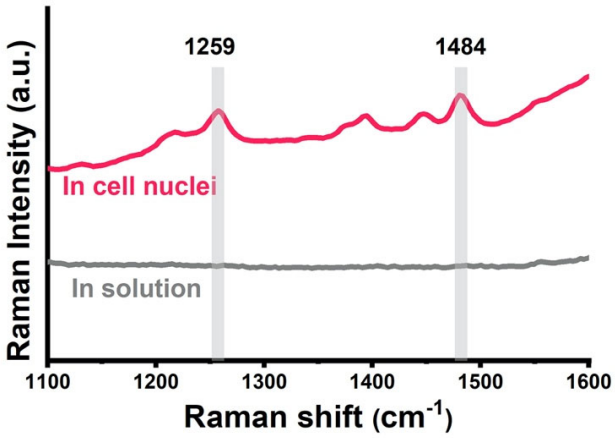

Figure S11. Enrichment of Raman signals of ActD at the effector site. Raman spectrum of 10 μM ActD in PBS solution (black trace) and in cell nuclei treated with 10 μM ActD (red trace). The characteristic peaks of ActD were detected in the cells treated with 10 μM ActD. However, we couldn't detect these peaks in the 10 μM ActD solution. This result demonstrates the difference of drug concentration in the medium and at the effector site.

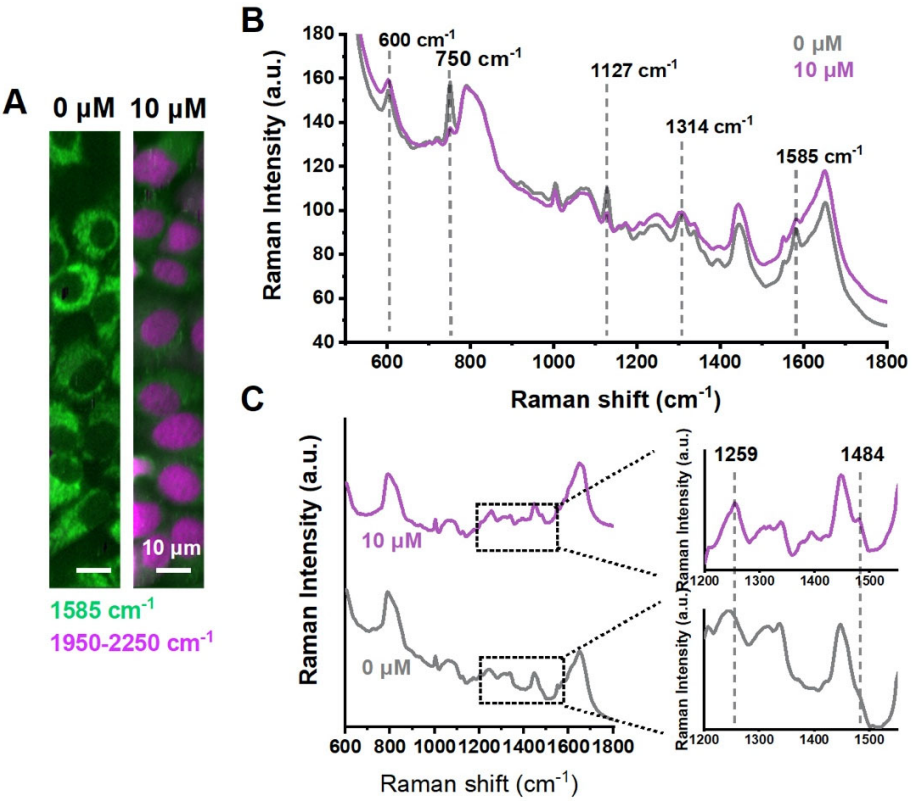

Figure S12. Hyperspectral Raman images of fixed HeLa cells. (A) Raman spectral images of HeLa cells treated with and without 10 μM ActD. The distribution of the 1585 cm^{-1} peak and average intensity of autofluorescence (1950-2250 cm^{-1}) were mapped to show cyt *c* and ActD, respectively. Scale bars, 10 μm. (B) The average spectra of cell cytoplasm treated with (purple trace) or without ActD (gray trace). A clear decline in all vibration modes (600 cm^{-1}, 750 cm^{-1}, 1127 cm^{-1}, 1314 cm^{-1}, and 1585 cm^{-1}) was observed. (C) The average spectra of cell nuclei treated with (purple trace) or without ActD (gray trace). The characteristic peaks of ActD at 1259 cm^{-1} and 1484 cm^{-1} were detected.

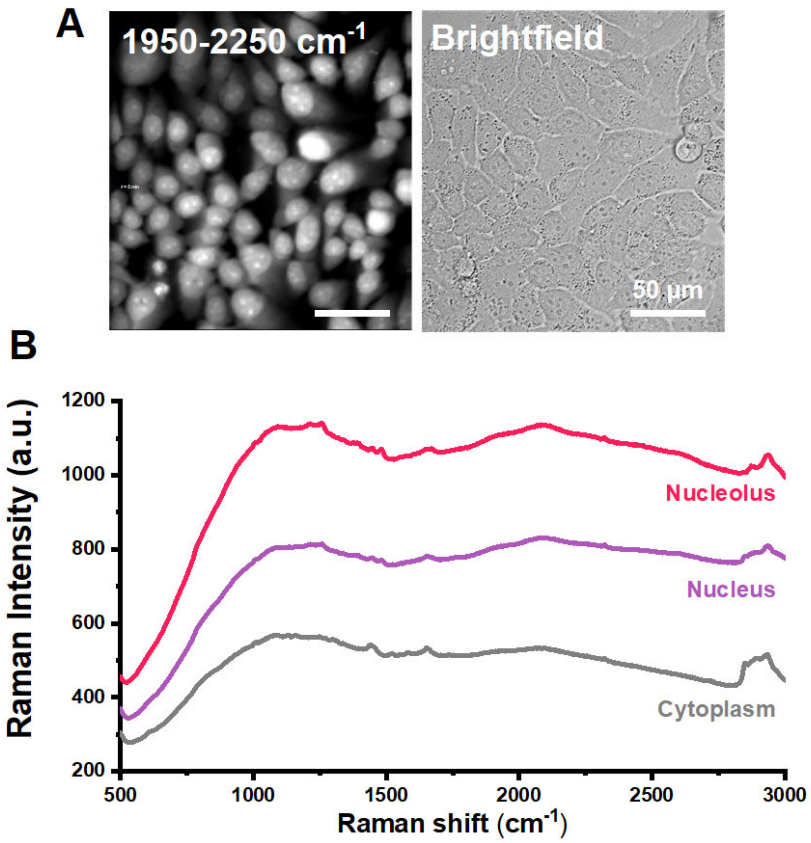

Figure S13. The fluorescence saturated faster in the nucleolus treated with 10 μM for 30 min. (A) The reconstructed Raman image using the cell-silent region (1950 cm^{-1} to 2250 cm^{-1}) and brightfield image demonstrate that the strongest fluorescent signal resembles the nucleolar structure. Scale bars, 50 μm. (B) Comparison of the fluorescent signal in the nucleolus, nucleus, and cytoplasm.

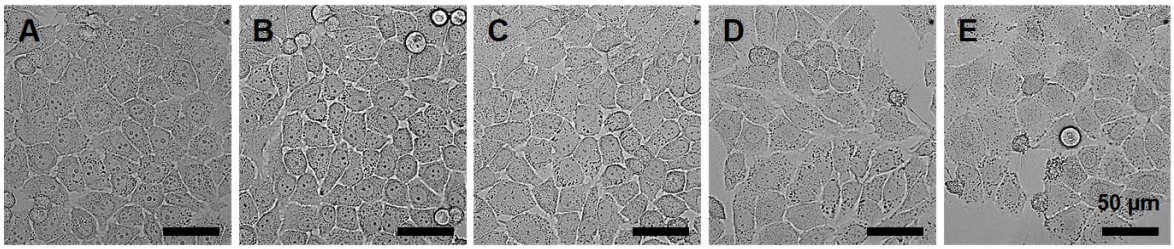

Figure S14. Nucleolus gradually disappear with the increase in incubation time. Before the ActD treatment (A) and after the treatment for 30 min (B), 1 h (C), 2h (D), and 4 h (E). Scale bars, 50 μm.

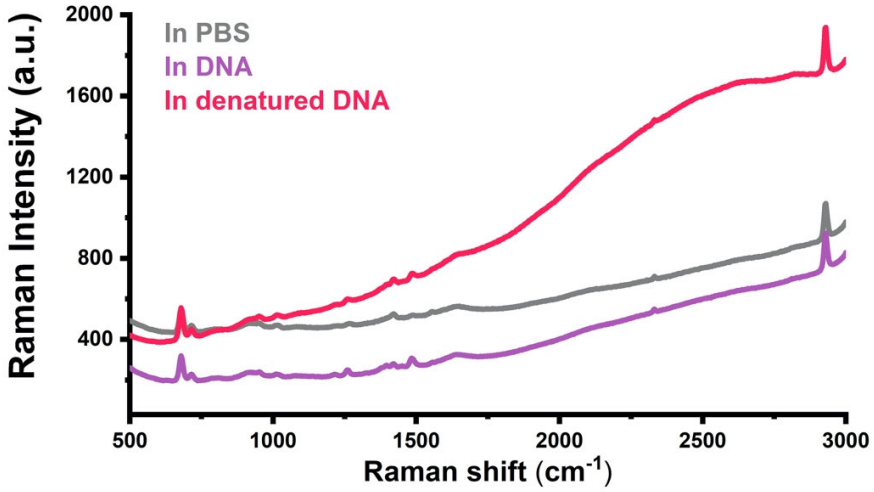

Figure S15. Binding with denatured DNA increases the fluorescence intensity of ActD. Comparison of the fluorescent signal of ActD in PBS (gray), DNA (purple), and denatured DNA (red). The peak of the shifted excitation maximum of fluorescence in denatured DNA is around 2600 cm^{-1}, which converted to wavelength is around 620 nm.